



Received: 17/11/2011
Accepted: 03/02/2012

Experimental and thermodynamic study of iron (30wt.%Cr) - base alloys containing between 2.5 and 5.0wt.% of carbon

P.Berthod*, M.Ba, A.Dia, L.Aranda
Institut Jean Lamour (CNRS UMR 7198), Faculté des Sciences et Technologies,
Université Henri Poincaré Nancy 1, Nancy-Université, Boulevard des Aiguillettes, BP
70239, F-54506 Vandoeuvre les Nancy, (FRANCE)
E-mail: Patrice.Berthod@ijl.nancy-universite.fr

Abstract

Six {Fe-30wt.%Cr}-based alloys containing from 2.5 to 5.0 wt.%C, were cast and heat treated during 50h for microstructure stabilization at 1000, 1100 and 1200°C. The melting ranges and the carbides' characteristics were experimentally characterized, and compared to the results of thermodynamic calculations. The microstructures are hypo-eutectic (2.5wt.%C), eutectic (3%C) and hyper-eutectic (3.5 to 5wt.%C), and the carbides are Cr₇C₃. The carbides fraction increases with the carbon content and tends to decrease with temperature. The carbon-richest alloys are hardened by more than 50vol.% of carbides. The results of thermodynamic calculations are consistent with the observed microstructures, but less with the fusion's temperature range. The obtained hardness, which can be higher than 800Hv, is favorable to a good wear behavior. Unfortunately it tends to decrease after exposure at 1200°C.

Keywords

Iron-chromium alloys; Chromium carbides; Experimental characterization; Thermodynamic calculations; Hardness.

Corresponding author's name and address

P.Berthod
Institut Jean Lamour (CNRS UMR 7198), Faculté des Sciences et Technologies,
Université Henri Poincaré Nancy 1, Nancy-Université, Boulevard des Aiguillettes, BP
70239, F-54506 Vandoeuvre les Nancy, (FRANCE)

INTRODUCTION

Carbon-containing iron alloys are generally known to possibly contain large quantities of hard phases able to bring high hardness to the alloys. The iron carbide Fe₃C (cementite) or the Fe₃C-containing eutectic compounds appeared at solidification in the common "white cast irons"^[1,2], the eutectoid { α + Fe₃C} compound (pearlite) present in some cast irons and in carbon steels^[3] and unstable phases obtained by quenching from the austenitic domain (martensite)^[4] are usual hard phases which can be easily obtained in iron-based alloys. If its chemical composition also contains chromium the iron alloy may reach high levels of hardness thanks to the formation of numerous interdendritic chromium carbides, as it can be

met in some iron-based bulk alloys^[5] or of hardfacing coatings^[6]. Simultaneous high levels of carbon and chromium may lead to bulk alloys, which are easy to elaborate by casting and which may display first high volume fractions of carbides for an enhanced hardness and wear resistance. They may also show a good resistance to high temperature oxidation in case of substantial increase in temperature during service (e.g. due to friction) with the presence of chromium, which is first a carbide-former element but also an element able to form protective oxide layers^[7].

A previous experimental and thermodynamic study concerning the microstructures stabilized at high temperatures dealt with ternary 30wt.%Cr-containing iron-

based alloys progressively enriched in carbon from 0 to 2wt.%C and elaborated by foundry^[8]. The topic of this study is to explore the microstructure behaviour at high temperature, and the resulting evolution of hardness, in the case of alloys containing higher carbon contents, from 2.5 to 5.0wt.%C, and thus higher carbide fractions. This work consists in the elaboration of alloys by foundry (to obtain typical solidified microstructures), the determination of their fusion temperature range (to keep an eye on possible difficulties of foundry manufacturability), and their characterization by several metallographic techniques after heat-treatments (to better know their microstructure behaviours in case of friction-caused heating for long times up to high temperatures). Finally these experimental results will be compared to predicted results issued from thermodynamic calculations.

EXPERIMENTAL

Synthesis, metallographic preparation and observations

Six alloys belonging to the Fe-30wt.%Cr-x%C family, "Fe25" (x=2.5), "Fe30" (3.0), "Fe35" (3.5), "Fe40" (4.0), "Fe45" (4.5) and "Fe50" (5.0) were cast under an inert atmosphere of 300mbar Ar, using a high frequency induction furnace (CELES), from pure elements (> 99.9%, Alfa Aesar). Fusion and solidification occurred in the cold copper crucible (cooled by internal water circulation) belonging to the furnace. The ingots, the masses of which were about 40g, were cut to bring samples with dimensions 2 × 2 × 8 mm³ destined to thermal analysis, and other samples with dimensions 10 × 10 × 3 mm³ to allow realizing the exposures to high temperature.

The as-cast microstructures of the alloys, and the microstructures of the samples subjected to heat-treatment, were examined on mounted and polished samples. To obtain them each ingot was cut in two parts using a Buehler Isomet 5000 precision saw. The obtained parts were embedded in {Araldite CY230 + Strengtheners Escil HY956} mixture, then polished. The embedded samples were polished using SiC papers under water (from 120 to 1200 grit), and thereafter with textile paper enriched with 1μm-abrasive particles until obtaining a mirror-like surface state. The metallographic observations were done using a XL30 Philips Scanning Electron Microscope (SEM), essentially in the Back Scattered Electrons mode (BSE). The used acceleration voltage was 20 kV. The chemical composition of each alloy was also controlled using a Cameca SX100 microprobe, by Wavelength Dispersion Spectrometry.

Thermal analysis

The solidus and liquidus temperatures were assessed by

Differential Thermal Analysis (DTA), using a Setaram TG-DTA apparatus, with an alumina crucible containing a cut part of the as-cast alloy. The thermal cycle was composed of a heating at 20 °C min⁻¹ from 20°C to 1200 °C, then at 5 °C min⁻¹ from 1200 to 1500 °C. After an isothermal 10 min.-stage at 1500°C the liquid alloy was cooled at -5 °C min⁻¹ from 1500 to 1200 °C, then at -20 °C min⁻¹ from 1200 to ambient temperature. These heat flux curves were exploited by reading the temperatures corresponding to the starts of fusion and of solidification, and the ones corresponding to the ends of fusion and of solidification.

Heat treatments and metallographic characterization

Three parts of each alloy were exposed at high temperature in a high temperature furnace in air: one at 1000°C, one at 1100°C and one at 1200°C. The heating was done at 20 °C min⁻¹ from 20°C to the targeted stage temperature, maintained at this constant temperature for 50 hours, and thereafter air-quenched. These parts of alloys were thereafter metallographically prepared as described above. X-Ray Diffraction measurements were performed on these mirror-like polished metallographic samples, using a Philips X-Pert Pro diffractometer (wavelength Cu Kα, 1.5406 Å) to identify the phases present in the alloys. The surface fractions of the carbides were measured by image analysis on {× 500}-micrographs taken using the SEM in the BSE mode on three locations randomly selected near the center of the initial ingot, using the Photoshop CS software of Adobe. The obtained values of surface fraction were considered close to the volume fractions.

Thermodynamic calculations

Thermo-Calc^[9] and a database containing the descriptions of the Fe–Cr–C system and of its sub-systems^[10-16] were used first to qualitatively explore the possible microstructures which can be met for the studied chemical compositions for the exposure temperatures (and eventually for some intermediate temperatures known by the alloys during the subsequent cooling).

Second, thermodynamic calculations allowed also identify the natures and quantitatively assess the mass fractions of the phases present at the thermodynamic equilibria at the three temperatures of heat treatment. These mass fractions were thereafter converted in volume fractions according to the following equation:

$$f_v[\varphi_j] = \frac{f_w[\varphi_j]}{\rho_{\varphi_j}} / \sum_i \left(\frac{f_w[\varphi_i]}{\rho_{\varphi_i}} \right)$$

in which $f_v[\varphi_j]$, $f_w[\varphi_j]$ and ρ_{φ_j} are respectively the volume fraction, the mass fraction and the density of the phase φ_j . The values used for the densities were 7.29 g/cm³ for

matrix (calculated with the measured masses and volumes of a binary Fe-30Cr sample), 6.97 g/cm³ for the Cr₂₃C₆ carbides and 6.92 g/cm³ for the Cr₇C₃ carbides^[17].

Third, Thermo-Calc was used to calculate the liquidus and solidus temperatures of the six alloys, for comparison with the DTA results.

Hardness measurements

Finally, the hardness of each alloy in all its heat-treated conditions was measured by Vickers indentations performed with an applied load of 30kg. The apparatus used was a Testwell Wolpert machine. The obtained values led in each case to an average value which was thereafter taken in consideration and to a standard deviation value which was used as uncertainty.

RESULTS

Preliminary exploration of the microstructures using Thermo-Calc

The possible microstructures were preliminarily explored using Thermo-Calc, for a chromium content of 30wt.% and over the [2.5; 5.0] weight carbon contents range. On the 30wt.%Cr-section of the Fe-Cr-C diagram presented in Figure 1, it appears first that the matrix of the alloys should be austenitic (FCC) for all the studied alloys at the three stage temperatures. Indeed the ferritic (BCC) type is seemingly possible at high temperature only for 30wt.%-containing alloys with carbon content lower than 2.4% C (at T higher than about 1100°C) and lower than 2.1wt.% for 1000 to 1200°C. The carbide present should be M₇C₃,

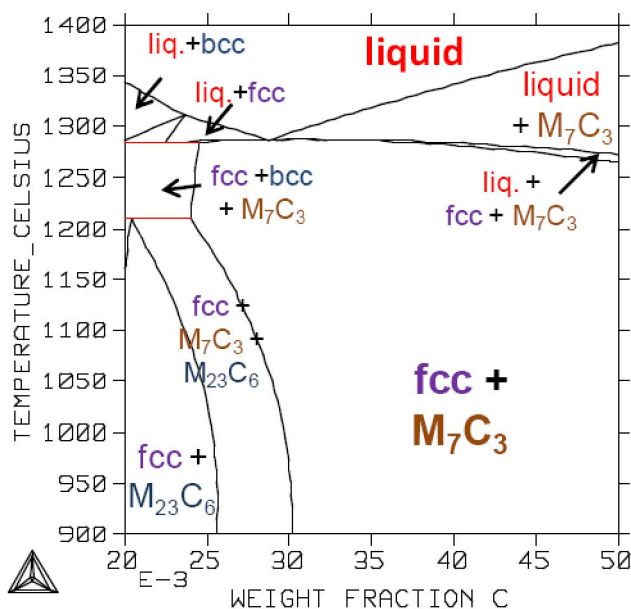


Figure 1 : Section at 30 wt.%Cr of the Fe-Cr-C diagram for the carbon content varying from 2.0 to 5.0wt.%, issued from Thermo-Calc calculations.

in most cases (Fe-30Cr-3.0C to Fe-30Cr-5.0C alloys at all temperatures). In the Fe-30Cr-2.5C alloy M₂₃C₆ may be the single carbide present at 1000°C and may co-exist with Cr₇C₃ at 1100 and 1200°C.

Concerning the type and repartitions of the carbides present just after solidification, all of them are eutectic M₇C₃ (mixed with matrix) in the Fe-30Cr-2.5C and Fe-30Cr-3.0C alloys, since the first one appears as a hypo-eutectic alloy and the second one as a near-eutectic alloy. For all the other ones, richer in carbon, solidification should obviously start by the crystallization of primary M₇C₃ carbides, followed by the eutectic part of solidification leading to a {FCC matrix + M₇C₃} eutectic compound, at a temperature which decreases when the carbon content in the alloy increases.

The theoretic natures and mass fractions of the carbides present in the six alloys according to Thermo-Calc are given in TABLE 1. M₂₃C₆ should be effectively the single carbide present in Fe25 at 1000°C, with a mass fraction of 42%. 100°C higher, the M₇C₃ are also present although M₂₃C₆ is still the main carbide. M₇C₃ is the single carbide present in the Fe25 alloy at 1200°C, as well as in all the other alloys at all the three temperatures. When the carbon content increases the mass fraction of M₇C₃ also increases, until reaching 53% in mass in Fe50 at 1000°C. When the considered temperature increases the M₇C₃ mass fraction loses only 3 mass.% of carbides between 1000 and 1200°C.

TABLE 1 : Natures and mass fractions of the phases present at 1000, 1100 and 1200°C for the targeted chemical compositions, according to Thermo-Calc calculations (matrix is of the {face centred cubic}-type for all alloys at all temperatures)

%mass	1000°C		1100°C		1200°C	
	Cr ₂₃ C ₆	Cr ₇ C ₃	Cr ₂₃ C ₆	Cr ₇ C ₃	Cr ₂₃ C ₆	Cr ₇ C ₃
Fe25	41.99	/	25.73	8.78	/	22.91
Fe30	/	31.32	/	29.96	/	28.25
Fe35	/	36.67	/	35.29	/	33.59
Fe40	/	42.03	/	40.67	/	38.99
Fe45	/	47.48	/	46.15	/	44.53
Fe50	/	53.07	/	51.80	/	50.27

As-cast microstructures and temperature ranges of fusion/solidification

The elaborated alloys display various as-cast microstructures as it can be seen in Figure 2 where they are illustrated. As indicated by Thermo-Calc calculations, the Fe25 alloy seems being effectively of the hypo-eutectic type since composed of primary dendrites of matrix and of a eutectic {matrix + carbides} compound in the interdendritic areas, Fe30 is obviously eutectic, and the C-richer alloys are all of the hyper-eutectic type with, in addition to the eutectic compound, additional coarse

primary carbides the quantity of which increases with the carbon content in the alloy.

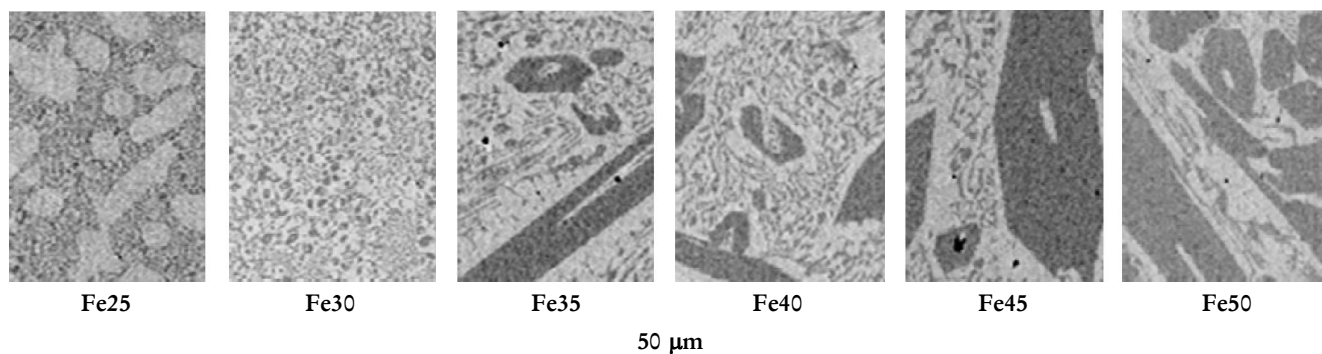


Figure 2 : The as-cast microstructures of all the six elaborated alloys (pictures taken with SEM in BSE mode).

The Differential Thermal Analysis technique was used to assess the real temperatures of fusion and solidification starts and ends, for the alloys in their as-cast conditions. The temperatures of fusion’s start, of solidification’s end and the average of the two former values were taken in consideration for the solidus temperature. In

the case of the liquidus temperatures it was the temperatures of fusion’s end, of solidification’s start and the average of the two former values. The two graphs plotted in Figure 3 present graphically the results, together with the solidus and liquidus temperatures calculated by Thermo-Calc.

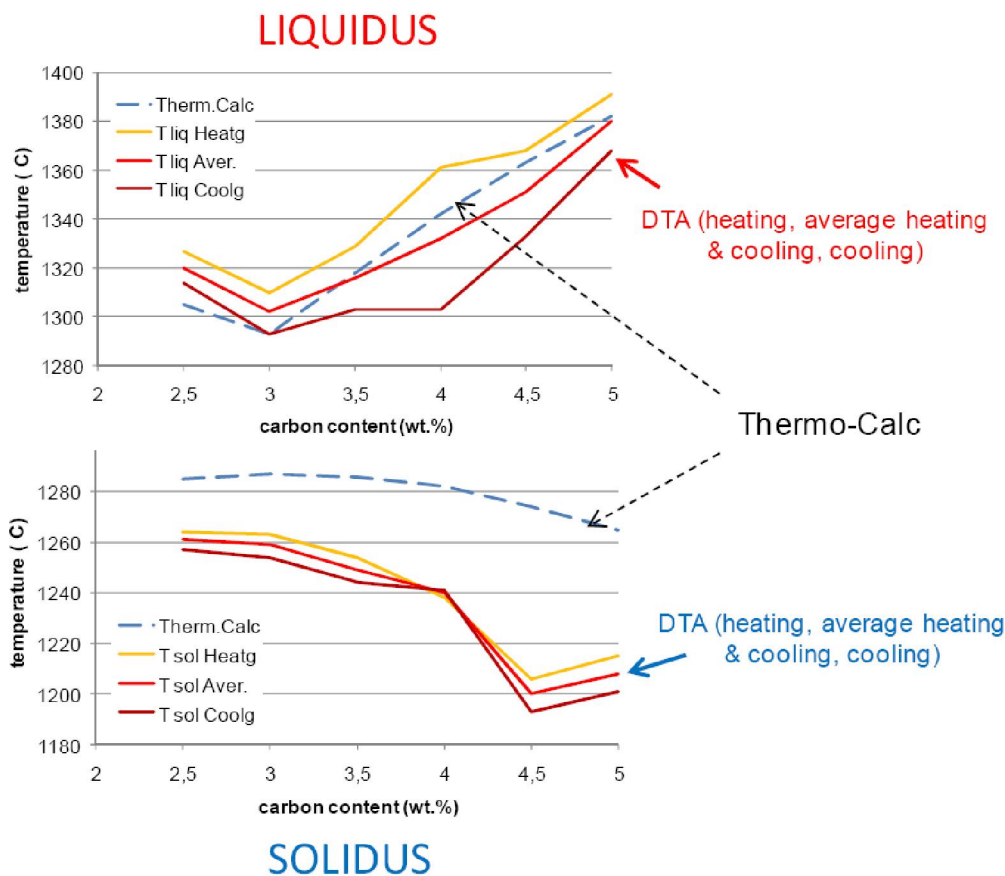


Figure 3 : Evolution of the liquidus (first graph, top) and solidus (second graph, bottom) temperatures with the carbon content; comparison of the values measured by DTA and the values calculated by Thermo-Calc (dotted lines)

One can see that there is globally a good agreement concerning the liquidus temperatures between measurements and calculations, for the evolution versus the carbon content (eutectic valley situated at about 3.0wt.% of carbon content (eutectic valley situated at about 3.0wt.% of carbon content (eutectic valley situated at about 3.0wt.% of carbon content (eutectic valley situated at about 3.0wt.% of carbon content) as well as for the values of temperature themselves. In contrast, there are

obviously serious discrepancies about the solidus temperatures since the mismatch of about 20-25°C increases to about 70°C for the carbon-richest alloys. It must be noticed that the Fe45 and Fe50 may start melting if exposed to 1200°C. With only 40°C more than 1200°C the Fe40 alloy is also possibly threatened by possible local melting.

It appears then preferable to expose to 1200°C only the three alloys with not too high carbon contents.

Characterization of the alloys' microstructures after heat-treatment

Three parts of each alloy were heat-treated at 1000 and 1100 and 1200°C* during 50 hours, a duration thought to be long enough for such high temperatures for allowing them to reach their thermodynamic equilibria (*: 1200°C only for the Fe25, Fe30 and Fe35 alloys). The cooling,

done by taking the heat-treated samples out the furnace and by letting them cooling in ambient air, was supposed to be fast enough to do not allow the alloys losing their high temperature carbides.

The microstructures of the heat-treated alloys are displayed in Figure 4 (Fe25, Fe30 and Fe35 at 1000, 1100 and 1200°C) and Figure 5 (Fe40, Fe45 and Fe50 at 1000 and 1100°C only). In all cases the microstructures after 50 hours at 1000 or 1100°C are very similar to the ones observed in the as-cast conditions (Figure 2). In contrast the alloys heat-

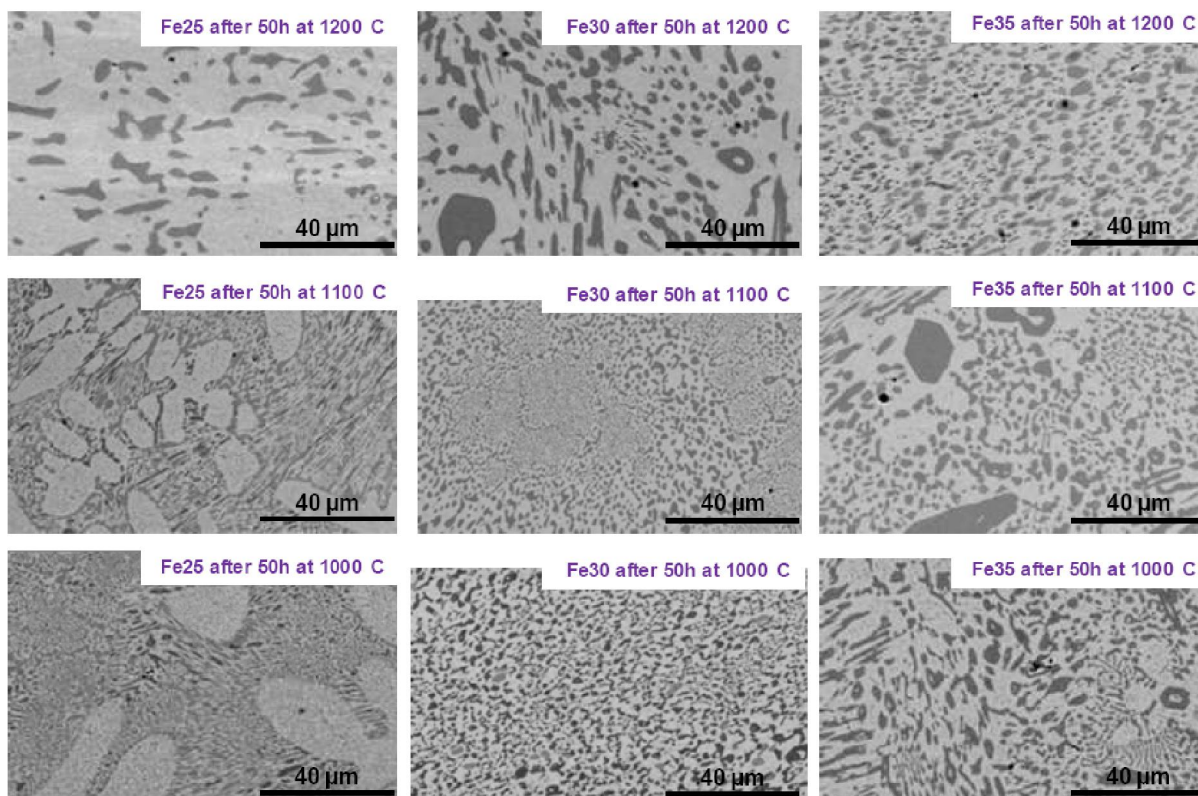


Figure 4 : Microstructures of the Fe-30Cr-2.5C, Fe-30Cr-3.0C and Fe-30Cr-3.5C alloys heat treated for 50 hours at 1000, 1100 and 1200°C (pictures taken with SEM in BSE mode).

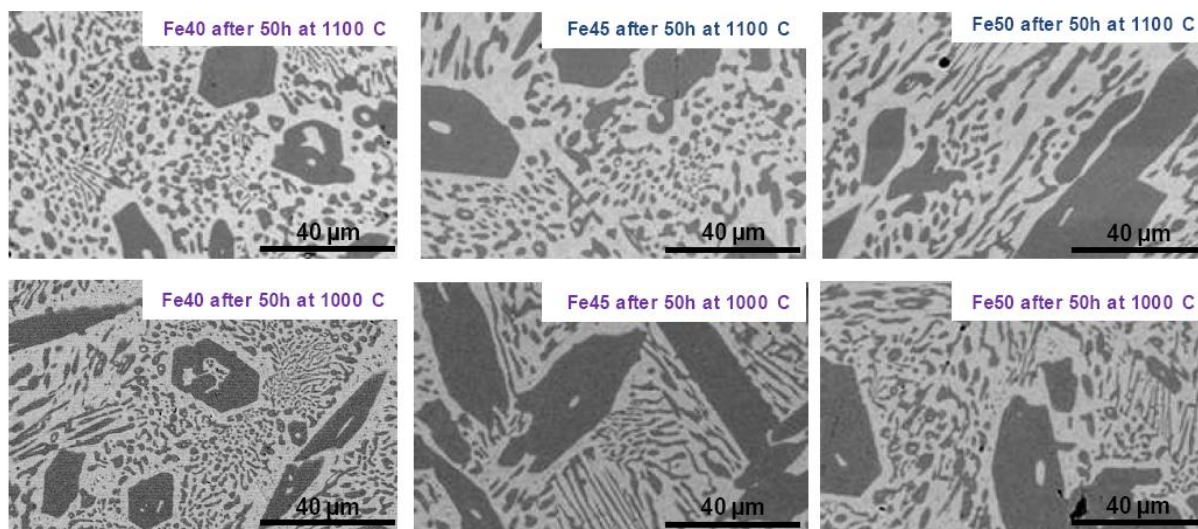


Figure 5 : Microstructures of the Fe-30Cr-4.0C, Fe-30Cr-4.5C and Fe-30Cr-5.0C alloys heat treated for 50 hours at 1000 and 1100°C (pictures taken with SEM in BSE mode).

treated at 1200°C (only Fe25, Fe30 and Fe35) are significantly changed: their carbides seem to be coarser and less numerous. In addition their surface fractions seem having decreased.

X-Ray Diffraction was performed on the heat-treated alloys and several of the obtained spectra are shown as examples in Figure 6 (Fe25 for the three temperatures), Figure 7 (Fe35 at all temperatures too) and in Figure 8 (Fe45 at 1000 and 1100°C). The higher peaks are logi-

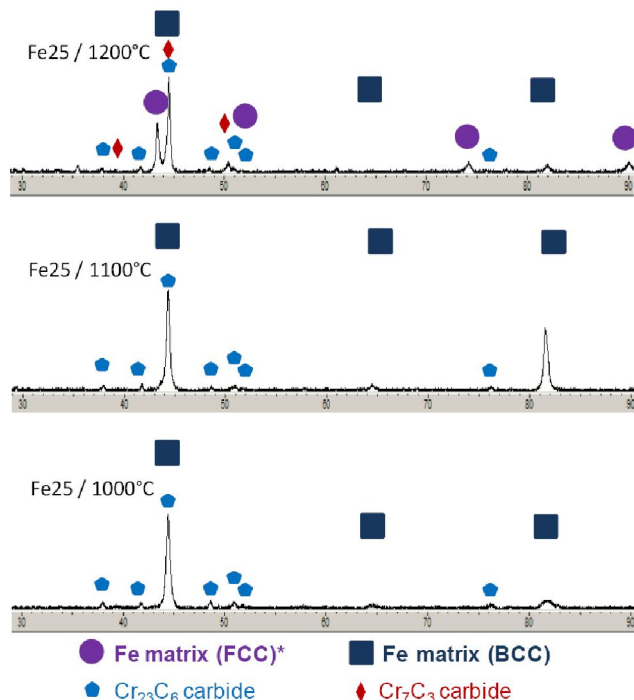


Figure 6 : X-ray diffraction spectra obtained on the Fe-30Cr-2.5C alloy in its three 50h-heat-treated states

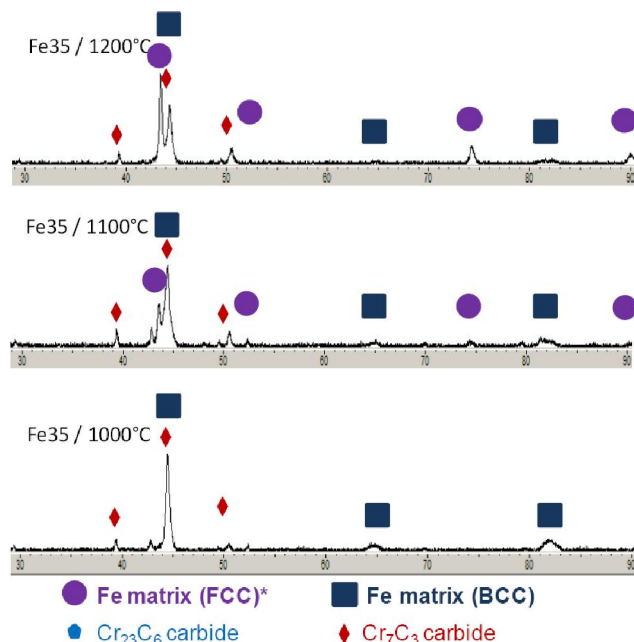


Figure 7 : X-ray diffraction spectra obtained on the Fe-30Cr-3.5C alloy in its three 50h-heat-treated states

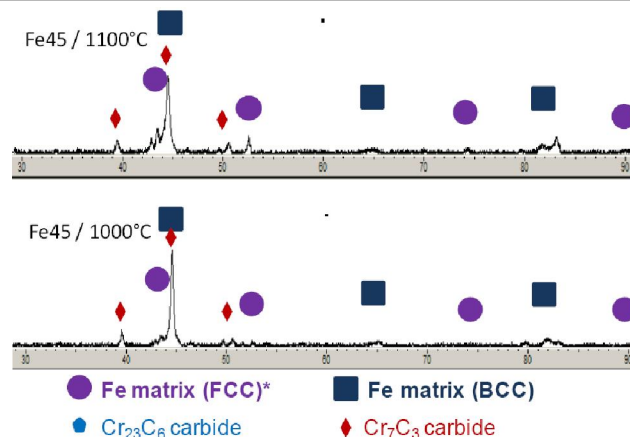


Figure 8 : X-ray diffraction spectra obtained on the Fe-40Cr-4.5C alloy in its two 50h-heat-treated states

cally associated to the matrix, which appear to be often of two types: essentially BCC for all alloy and all temperatures, mixed with a second form in some cases: FCC which is the crystallographic network predicted for matrix at the three high temperatures of heat-treatment. One must notice that the peaks associated to the FCC matrix were found to be slightly shifted on the right by comparison with the usual angles for pure FCC Fe, maybe because of the presence of Cr in substitution (Cr is a slightly smaller atom than Fe).

Unfortunately the main peaks of BCC and FCC correspond to the same angle as the main theoretic peaks of the carbides. However it was possible to identify the carbides. The main ones present in the Fe25 alloy heat-treated at 1000°C or 1100°C are all Cr_{23}C_6 while the two carbides Cr_{23}C_6 and Cr_7C_3 co-exist in the Fe25 alloy heat-treated at 1200°C (Figure 6). In the other alloys, richer in carbon, Cr_{23}C_6 is not present any more and Cr_7C_3 seems being the single carbide. The intensities of the peaks associated to this Cr_7C_3 carbide globally rise when the carbon content in the alloy increases, while new supplementary small peaks appear. These ones are too small and too numerous to be easily indexed but it seems that Cr_3C_2 can be also present in the C-richer alloys.

Surface fractions of carbides determined by image analysis; comparison with thermodynamic calculations

Three SEM/BSE micrographs were taken at $\times 1000$ per heat-treated alloy. They were analyzed by image analysis using the Adobe Photoshop CS software and the surface fractions of carbides were estimated by the obtained average value, while the standard deviation was taken as uncertainty. Thermo-Calc calculations were performed in parallel to know the natures and the volume fractions (after conversion of the mass fractions) of the phases present at the thermodynamic equilibrium at 1000, 1100 and

1200°C* (*: only for Fe25 to Fe35). The results are given in TABLE 2.

TABLE 2 : Natures (XRD) and surface fractions (Image Analysis) of carbides in the Fe25, Fe30 and Fe35 alloys heat-treated at 1000, 1100 and 1200°C; comparison with Thermo-Calc results

% vol.	1000°C		1100°C		1200°C	
	Cr ₂₃ C ₆	Cr ₇ C ₃	Cr ₂₃ C ₆	Cr ₇ C ₃	Cr ₂₃ C ₆	Cr ₇ C ₃
exp.	36.8 ± 2.2	4.6 ± 1.5	25.2 ± 0.7	6.5 ± 1.7	/	23.1 ± 0.4
Fe25	∧	∨	∧	∧	OK	∧
calc.	43.1	/	26.5	9.1	/	23.8
exp.	11.12 ± 2.9	20.6 ± 2.3	/	28.8 ± 4.5	/	28.4 ± 2.2
Fe30	∨ ∨	∧ ∧	OK	OK	OK	OK
calc.	/	32.5	/	31.1	/	29.3
exp.	/	41.2 ± 2.5	/	36.1 ± 0.9	/	31.8 ± 0.1
Fe35	OK	∨	OK	OK	OK	∧
calc.	/	37.9	/	36.5	/	34.8
exp.	/	44.2 ± 3.6	/	42.9 ± 3.6		
Fe40	OK	OK	OK	OK		
calc.	/	43.3	/	41.9		
exp.	/	50.8 ± 1.3	/	42.4 ± 3.8		
Fe45	OK	∨	OK	∧	Not done	
calc.	/	48.8	/	47.4		
exp.	/	55.9 ± 6.9	/	50.3 ± 6.80		
Fe50	OK	OK	OK	OK		
calc.	/	54.4	/	53.1		

The carbides present in the Fe25 are of two types after heat-treatment at 1000 and 1100°C: the Cr₂₃C₆ (the greatest part) which are darker than matrix because of their lower average atomic mass, and the Cr₇C₃ darker than the Cr₂₃C₆ since they contain a higher atomic percentage of carbon. There is thus a little mismatch between experiment and calculations concerning the carbides natures at 1000°C but the calculated M₂₃C₆ fraction well correspond to the sum {Cr₂₃C₆ + Cr₇C₃} of surface (or volume) experimental fractions. At 1100°C, the two carbides types were well predicted by Thermo-Calc but the cumulated volume fractions lead to a value significantly higher than measured by image analysis. For 1200°C the agreement is very good. For Fe30 heat-treated at 1000°C two carbides are present (Cr₇C₃ but also Cr₂₃C₆) but their sum of surface fractions well correspond to calculations. The {calculation-experiment} agreement is good for the same alloy at the two highest temperatures. The agreement is also good globally for the Fe35 alloy, as well as for the three carbon-richest alloys at 1000 and 1100°C.

Hardness measurements

Vickers indentations were performed on the heat-treated alloys in an area close to the center of the initial ingot. The average of all the obtained values for each heat-treated

alloy and the accompanying standard deviation are given in TABLE 3. It appears first that there was a significant dispersion of the results since the standard deviation is often of several tens of hardness points. Second, globally, for the alloys not really affected by the heat-treatment (stage temperature of 1000 or 1100°C) the hardness is of a very high level, around 700-800 Hv. For a given temperature of the applied heat-treatment, hardness does not really depend on the carbon content, but an increase in temperature tends to lower hardness, especially between 1000/1100°C and 1200°C (alloys Fe25, Fe30 and Fe35). However the hardness of the concerned alloys remains at a high level (400-500 Hv).

TABLE 3 : Hardness of the heat-treated alloys (Hv30kg)

Hv30kg	1000°C	1100°C	1200°C
Fe25	833 ± 33	815 ± 25	416 ± 35
Fe30	721 ± 34	827 ± 58	489 ± 8
Fe35	728 ± 31	836 ± 24	511 ± 32
Fe40	770 ± 37	822 ± 35	
Fe45	824 ± 16	707 ± 31	Not done
Fe50	824 ± 32	771 ± 13	

DISCUSSION

The enrichment with carbon of a Fe-30Cr base beyond 2wt.% obviously leads to more carbides in the alloys. In addition, the supplementary carbon progressively added to the Fe-30Cr base is entirely used to form carbides, even up to 5wt.%C. This allows the microstructures displaying very high carbides fractions (more than 55% of the alloy in volume in Fe50 heat-treated at 1000°C). Contrarily to what occurs in the Ni-30Cr-C system^[18], no graphite appears beyond a critical carbon content and the progression of the carbide fraction is never stopped. Further, there is a single carbide type over almost the whole carbon range studied here for the three temperatures of heat treatment: Cr₇C₃, more precisely M₇C₃ with M being mainly Cr (2-3 times more Cr than Fe in atomic percent, according to Thermo-Calc results). Another carbide was also met, Cr₂₃C₆, only in the Fe25 alloy, which marks a transition between the Fe30 to Fe50 alloys and the Fe-30Cr-xC alloys earlier studied^[8] which all contained Cr₂₃C₆ carbides at these temperatures.

In fact, other carbides are suspected to be present in the carbon-richest alloys, as revealed by X-ray diffraction. It seems that, despite that the alloys were air-quenched at the end of the heat-treatments, the cooling was apparently not fast enough to totally obstruct the possible transformations of the high temperature carbides (Cr₇C₃) in other carbides more stable at intermediate temperatures. According to supplementary calculations performed with

Thermo-Calc it effectively appears that the Cr_3C_2 type may appear near 600-500°C to partly replace the Cr_7C_3 in the Fe35, Fe40 and Fe45, and wholly for Fe50. Even they were a little detected by XRD, such carbides were not observed with the SEM.

In contrast, in some heat-treated samples the matrix type has wholly become ferritic. In most cases a residual part of austenitic matrix was also detected by X-ray diffraction, the most often after cooling from the highest heat-treatment temperatures. The total FCC \rightarrow BCC transformation, as is to say of the matrix crystallographic network stable at high temperature to the one stable at room temperature, is effectively predicted by Thermo-Calc near 900-700°C for these alloys.

Globally, the thermodynamic calculations performed with the database described earlier in the text, have here correctly predicted the microstructures of the studied alloys for the three high temperatures of interest, as it resulted here from comparison with XRD and image analysis of surface fractions. However it must be noted that the C-richest alloys, which contain a significant proportion of coarse pro-eutectic carbides, led first to problems of microstructural homogeneity often leading to dispersion of results and high values of standard deviation. Second, the presence of so elongated carbides possibly led to a worse equivalence between surface fractions and volume fractions. Concerning the melting ranges, calculations led to liquidus determinations consistent with the DTA experiments. In contrast the solidus temperature was overestimated, with the risk of exposing the less refractory alloys to long time at temperature which may induce a melting beginning.

As consequence of the high carbides fractions allowed by the absence of graphite appearance and of change to C-richest carbides, the volume fractions can reach very high values, which remain almost constant even after several tens of hours spent at 1000 or 1100°C. With such proportions of very hard particles (1650Hv for the $Cr_{23}C_6$ of Fe25 and 1336 Hv for the Cr_7C_3 of all the other alloys^[19]) this allows thinking to very high levels of hardness at high temperature. They are probably lower than values measured here at room temperature but they may be improved at high temperature by the fact that matrix should be austenitic instead essentially ferritic at ambient temperature.

CONCLUSION

The Fe-30Cr-xC ($x=2.5$ to 5wt.%) system offers bulk materials very hard but with a ductile matrix favourable to toughness, not expensive since easy to elaborate (foundry) and requiring more or less cheap pure elements

(iron-based). Chromium carbides do not really evolve at less than 1100°C and they can play as chromium reservoirs to ensure a good resistance against hot oxidation and corrosion, probably much better than alloys hardened by more oxidizable particles as tungsten carbides. Such alloys appear suitable as pieces for applications requiring both wear resistance and heat resistance. It can be interesting to extend this experimental exploration to carbon contents higher than 5wt.%C, to discover an eventual limit of carbon content beyond which a new phase, possibly detrimental for hardness, may appear, and then the maximal volume fraction of carbide that is possible to reach.

ACKNOWLEDGEMENT

The authors thank the Electron Microscopy and Microanalysis Common Service of the Faculty of Sciences and Technologies of Nancy, as well as Thierry Schweitzer for his technical assistance and Pascal Villegier for the XRD measurements.

REFERENCES

- [1] G.Lesoult; 'Solidification: Cristallisation et Microstructures', Techniques de l'ingénieur, Paris, (1986).
- [2] W.Kurz, D.J.Fisher; 'Fundamentals of Solidification', Trans. Tech. Publ., Switzerland, (1989).
- [3] M.Durand-Charre; 'Microstructure of Steels & Cast Irons', Springer, (2004).
- [4] A.Litwinchick, F.X.Kayser, H.H.Baker, A.Henkin; *J.Mater. Sci.*, **11**, 1200 (1976).
- [5] H.E.N.Stone; *J.Mater.Sci.*, **14**, 2781 (1979).
- [6] B.V.Cockeram; *Met.Mater.Trans.A: Phys.Met.Mater.Sci.*, **33**, 3403 (2002).
- [7] D.Young; 'High Temperature Oxidation and Corrosion of Metals', Elsevier Corrosion Series, Amsterdam, (2008).
- [8] P.Berthod, P.Lemoine, J.Ravaux; *Int.J.Mat.Res.(formerly Z.Metallkd.)*, **99**, 964 (2008).
- [9] Thermo-Calc version N; 'Foundation for Computational Thermodynamics', Stockholm, Sweden, <http://www.thermocalc.com>; Copyright (1993), (2000).
- [10] A.Fernandez Guillermet, P.Gustafson; *High Temp.High Press*, **16**, 591 (1984).
- [11] J.-O.Andersson; *Int.J.Thermophys.*, **6**, 411 (1985).
- [12] P.Gustafson; *Carbon*, **24**, 169 (1986).
- [13] J.-O.Andersson, B.Sundman; *Calphad*, **11**, 83 (1987).
- [14] P.Gustafson; *Scan.J.Metall.*, **14**, 259 (1985).
- [15] J.-O.Andersson; *Calphad*, **11**, 271 (1987).
- [16] J.-O.Andersson; *Met.Trans.A*, **19A**, 627 (1988).
- [17] P.T.B.Shaffer; 'Handbooks of High-Temperature Materials N°1. Materials Index', Plenum Press, New York, (1964).
- [18] P.Berthod, E.Souaillat, O.Hestin, P.Lemoine Th.Schweitzer; *Ann.Chim.Sci.Mat.*, **35**, 291 (2011).
- [19] G.V.Samsonov; 'High-Temperature. Materials Properties Index', Plenum Press, New York, (1964).